Intracellular calcium concentration changes initiated by *N*-methyl-D-aspartic acid receptors in retinal horizontal cells

Xu-Long Wang, Xiao-Dong Jiang and Pei-Ji Liang

Shanghai Jiao Tong University, Shanghai, China

Correspondence to Pei-Ji Liang, D. Phil, School of Life Science and Biotechnology, Shanghai Jiao Tong University, 800 Dong-Chuan Road, Shanghai 200240, China
Tel: +86 21 34204015; fax: +86 21 34204016; e-mail: pjliang@sjtu.edu.cn

Received 26 January 2008; accepted 3 February 2008

Intracellular calcium concentration changes initiated by *N*-methyl-D-aspartic acid receptors were studied in carp retinal horizontal cells. Fura-2 fluorescent calcium imaging showed that HI subtype horizontal cells responded to exogenously applied *N*-methyl-D-aspartic acid with a transient intracellular free Ca^{2+} ($[Ca^{2+}]_i$) increase that decayed to a sustained, but elevated level of $[Ca^{2+}]_i$. Contributions of different Ca^{2+} flux pathways underlying the time course of this increase in $[Ca^{2+}]_i$ were explored via experiment as well as via a computational model based on the biophysical properties of HI cells. Intracellular calcium stores were suggested to play crucial role in the initial transient increase of $[Ca^{2+}]_i$. *NeuroReport* 19:675–678 © 2008 Wolters Kluwer Health | Lippincott Williams & Wilkins.

Keywords: calcium imaging, computational model, *N*-methyl-D-aspartic acid receptors, retina

Introduction

Calcium is one of the most versatile intracellular messengers playing crucial roles in many signal transduction processes [1]. Horizontal cells (HCs) are second-order neurons of the vertebrate retina, which are responsible for the lateral interaction of signal transmission between photoreceptor and bipolar cells [2]. Intracellular free Ca^{2+} ($[Ca^{2+}]_i$) of HCs can be affected by a number of factors including activation of calcium-permeable glutamate receptors and voltage-gated Ca^{2+} channels, cytoplasmic Ca^{2+} buffering by Ca^{2+}-binding proteins, and active transport by the membrane Na^+/Ca^{2+} exchangers and Ca^{2+} pumps, etc. Furthermore, HCs in teleost retina possess ryanodine-sensitive calcium stores on endoplasmic reticulum (ER) membrane, which contribute to $[Ca^{2+}]_i$ changes through calcium-induced calcium release (CICR) [3,4].

Ionotropic glutamate receptors have been classified as *N*-methyl-D-aspartic acid (NMDA) and non-NMDA subtypes, with the latter being further divided into α-amino-3-hydroxy-5-methyl-4-isoxazole propionic acid (AMPA) and kainate receptors [5]. In the vertebrate retina, fast excitatory synaptic activation in the HCs is generally believed to be mediated by AMPA-type glutamate receptors [6]. In contrast, it was recently reported that functional NMDA receptors are expressed in cone-driven HCs (H1 cells) of carp retina [7]. In this study, changes in cytoplasmic $[Ca^{2+}]_i$ induced by exogenous application of NMDA were investigated in freshly dissociated H1-type HCs of carp retina using a fura-2-based Ca^{2+} imaging technique. A computational model of H1 cell was also constructed to quantitatively explore how the Ca^{2+} regulation mechanisms interact with each other to give rise to the time course of $[Ca^{2+}]_i$ changes observed in the experiment.

Materials and methods

Physiological experiments

Cell dissociation

HCs were dissociated from retinas of adult carp (*Carassius auratus*, 15–20 cm body length). The cell preparation procedure was carried out by following the description in a previous report [3]. The retina was incubated for 30 min at 25°C in Hank's solution (in mM: 120.0 NaCl, 3.0 KCl, 0.5 $CaCl_2$, 1.0 $MgSO_4$, 1.0 Na-pyruvate, 1.0 NaH_2PO_4, 0.5 $NaHCO_3$, 20.0 *N*-2-hydroxyl piperazine-*N*′-2-ethane sulfonic acid (HEPES) and 16.0 glucose), which contained 25 U/ml papain (E. Merck, Germany) and 1 mg/ml L-cysteine (Bo'ao, China). To obtain dissociated HCs, retina pieces were gently triturated with fire-polished glass pipettes in normal Ringer's solution (in mM: 120.0 NaCl, 5.0 KCl, 2.0 $CaCl_2$, 1.0 $MgCl_2$, 10.0 HEPES and 16.0 glucose). The cell suspension was moved to the recording chamber for calcium imaging recording.

Calcium imaging

Fura-2 AM (Dojindo, Japan) was added to prepared cell suspension to reach a final concentration of 5 μM. Cells in the suspension were incubated at 25°C for 15 min to allow for adherence to the base of the recording chamber and fura-2 loading, and then continuously perfused with Mg^{2+}-free Ringer's solution before recording. H1 cells were identified by their characteristic morphology as having round soma

with extended, stubbly dendrites [8]. A high-speed scanning polychromatic light source was used for alternate excitations at wavelengths of 340 and 380 nm. The relevant fluorescence image pairs (F340 and F380) were acquired every 2 s by a digital CCD camera (C4742-95-12NRB; Hamamatsu, Japan), and $[Ca^{2+}]_i$ was indexed by the ratio value of F340/F380.

Computational model

Computational simulations were carried out using NEURON software (Yale University, USA) [9]. A single cylindrical cable neuron was constructed. The diameter and length of the model neuron were chosen to be 20 and 22.5 μm, respectively, such that the internal volume and surface area of the cylindrical neuron matched those of a hemispherical neuron with 15 μm radius, which is the typical geometry of H1 cells in our experiment. Detailed equations describing biophysical processes are given in the appendix. A schematic illustration of our model is presented in Fig. 1.

Results

N-methyl-D-aspartic acid-receptor-initiated $[Ca^{2+}]_i$ changes in H1 cells

The time course of $[Ca^{2+}]_i$ changes recorded from an H1 cell is plotted in Fig. 2. The application of 100 μM NMDA in the presence of 50 μM glycine, which is a coagonist of NMDA receptors [7], induced a swift increase in $[Ca^{2+}]_i$. The ratio value of F340/F380 increased from a base level of 0.45 to a peak level of 0.95 within 10 s. This increase was transient and the ratio value then gradually decreased to a steady level of 0.72 over a period of about 30 s. Consistent results were observed in seven H1 cells. Ratio values for periods of initial steady state before drug application, peak response and final steady state in response to exogenously applied NMDA are averaged in the inset. Changes in individual neurons are indicated by solid lines. Furthermore, the NMDA-induced increase in $[Ca^{2+}]_i$ was completely eliminated in the presence of 100 μM AP-5, a competitive antagonist of NMDA receptors (similar results were observed in three neurons).

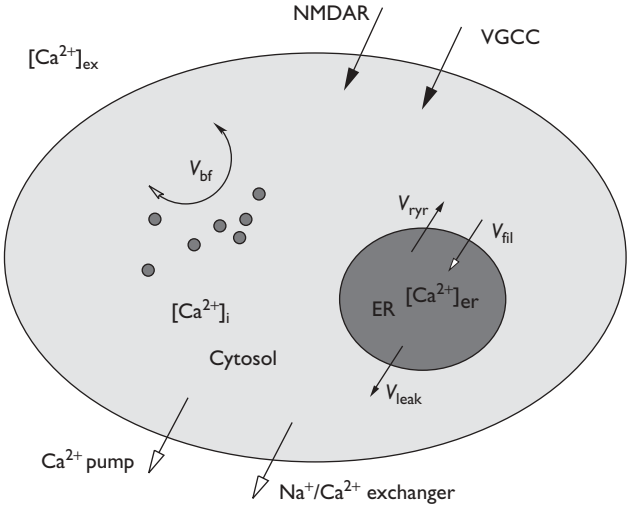

Fig. 1 General scheme of the main processes involved in $[Ca^{2+}]_i$ changes. ER, endoplasmic reticulum; NMDAR, *N*-methyl-D-aspartic acid receptor; V_{bf}, binding of Ca^{2+} to Ca^{2+} buffer proteins; V_{fil}, transport of Ca^{2+} into the ER by ER Ca^{2+} pump; VGCC, voltage-gated calcium channel; V_{ryr}, Ca^{2+} release from the ER through ryanodine receptor activation; V_{leak}, leak fluxes of Ca^{2+} across the ER membrane.

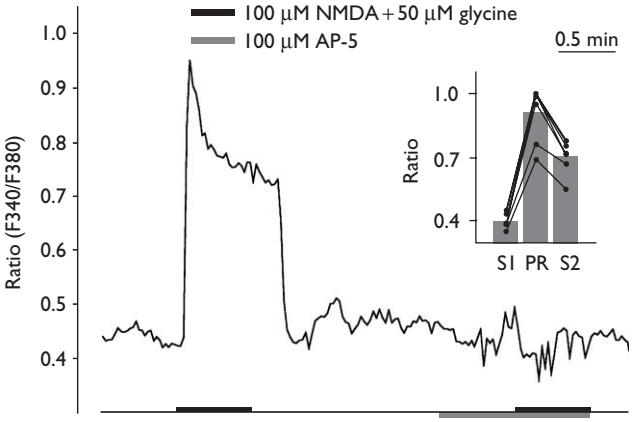

Fig. 2 *N*-methyl-D-aspartic acid (NMDA)-induced $[Ca^{2+}]_i$ response in HI cells. When NMDA together with glycine was applied, a transient increase of $[Ca^{2+}]_i$ was induced. In the presence of AP-5, NMDA failed to trigger significant $[Ca^{2+}]_i$ increment. Inset: averaged ratio values obtained from seven cells recorded during initial steady (SI), peak response (PR) and final steady (S2) states. Solid lines represent data obtained from individual neurons.

Table 1 Parameter values of model equations for Ca^{2+}-related physiological mechanisms

Physiological mechanism	Parameter value	Unit
NMDA conductance	K_f=0.072	$mmol^{-1}/l^{-1}/ms$
	K_b=0.0066	ms^{-1}
	$\bar{g}_{NMDA}$ = 1.2	mS/cm^2
Voltage-gated Ca^{2+} conductance	K_{Ca}=0.3	μmol/l
	τ_{Ca}=2.86	s
	$\bar{g}_{Ca}$ = 12	$\mu S/cm^2$
Ca^{2+} pump	A_{pump}=0.068	$pmol/cm^2/ms$
	K_{pump}=5e^{-4}	mmol/l
Na^+/Ca^{2+} exchanger	K_{ex}=0.747	$nA/mmol^4/cm^2$
	r=0.59	
Ca^{2+} processes on ER	v_{ryr}=0.013	ms^{-1}
	v_{fil}=0.00048	mmol/l/ms
	v_{leak}=0.001	ms^{-1}

ER, endoplasmic reticulum.

Computational model of *N*-methyl-D-aspartic acid-triggered changes in $[Ca^{2+}]_i$

Using parameter values listed in Table 1, the simulated time course of increase in $[Ca^{2+}]_i$ is plotted in Fig. 3a (solid line). To illustrate relative roles of mechanisms related to the $[Ca^{2+}]_i$ changes, simulated results of Ca^{2+} current mediated by each individual component are plotted separately in Fig. 3b. The positive currents reflect Ca^{2+} efflux from cytoplasm to external environment or Ca^{2+} refill from cytoplasm to ER. The modelling results show that NMDA conductance mediates a sustained calcium influx. Voltage-gated Ca^{2+} conductance is also activated after the membrane potential changes. Ca^{2+} efflux on the cell membrane is mediated by Ca^{2+} pumps and Na^+/Ca^{2+} exchangers. Ca^{2+} exchanges between ER and cytoplasm are mediated by the ryanodine-receptor-mediated CICR, ATPase-mediated Ca^{2+} refill and Ca^{2+} leakage. The negative Ca^{2+} flow across the ER

membrane, which gradually decreases as indicated by the shadow in Fig. 3b, is responsible for the initial transience of $[Ca^{2+}]_i$ changes as suggested by our simulation results. When the ER-mediated Ca^{2+} exchanges are eliminated from the model, no transient increase can be generated in the model neurons $[Ca^{2+}]_i$ changes in response to NMDA application, as illustrated in Fig. 3a (dotted line).

Experimental result of endoplasmic reticulum effect on the *N*-methyl-D-aspartic acid-initiated $[Ca^{2+}]_i$ changes

Appendix

The status of NMDA receptors can be described according to the following equations:

$$\begin{aligned} \frac{dR_o}{dt} &= K_f \cdot T \cdot R_c - K_b \cdot R_o \\ R_o + R_c &= 1 \end{aligned} \quad (1)$$

where R_c and R_o represent the percentage of closed and open states of the NMDA receptors, respectively; T is the concentration of NMDA; K_f and K_b are the rate constants for transmitter binding and unbinding processes, respectively. The NMDA-mediated current is further divided into Ca^{2+} current [$I_{NMDA}(Ca^{2+})$] and nonspecific ion currents [$I_{NMDA}(X)$]:

$$\begin{aligned} I_{NMDA}(Ca^{2+}) &= \bar{g}_{NMDA} \cdot R_o \cdot f_{Ca} \cdot (V_m - E_{Ca}) \\ I_{NMDA}(x) &= \bar{g}_{NMDA} \cdot R_o \cdot (1 - f_{Ca}) \cdot (V_m - E_x) \end{aligned} \quad (2)$$

where $\bar{g}_{NMDA}$ is the maximal conductance of NMDA receptors; f_{Ca} represents the Ca^{2+} fraction of the NMDA conductance [13].

Ca^{2+} current through the voltage-gated Ca^{2+} conductance can be described as:

$$\begin{aligned} I_{Ca} &= \bar{g}_{Ca} \cdot m_{Ca} \cdot h_{Ca} \cdot (V_m - E_{Ca}) \\ \frac{dm_{Ca}}{dt} &= \alpha m_{Ca} \cdot (1 - m_{Ca}) - \beta m_{Ca} \cdot m_{Ca} \\ h_{Ca} + \tau_{Ca} \frac{dh_{Ca}}{dt} &= K_{Ca}^n / (K_{Ca}^n + [Ca^{2+}]_i^n) \end{aligned} \quad (3)$$

where $\bar{g}_{Ca}$ is the maximal conductance of voltage-gated Ca^{2+} channel; m_{Ca} and h_{Ca} represent the activation and inactivation variables, respectively; K_{Ca} is the half-inactivation parameter; α and β are forward and backward rate coefficient, respectively [4].

Ca^{2+} flux mediated by Ca^{2+} pumps can be described as:

$$flux_{pump} = \frac{A_{pump} \cdot [Ca^{2+}]_i}{K_{pump} + [Ca^{2+}]_i} \quad (4)$$

where A_{pump} is the maximal pumping rate and K_{pump} is the dissociation constant [4].

Current carried by Na^+/Ca^{2+} exchangers can be described as:

$$I_{ex} = K_{ex} \cdot \left\{ \begin{array}{l} [Na^+]_i^3 \cdot [Ca^{2+}]_o \cdot \exp\left(r \cdot V_m \cdot \frac{F}{RT}\right) \\ -[Na^+]_o^3 \cdot [Ca^{2+}]_i \cdot \exp\left[-(1-r) \cdot V_m \cdot \frac{F}{RT}\right] \end{array} \right\} \quad (5)$$

where K_{ex} is a scaling coefficient; F, R and T are the Faraday constant, the gas constant and the absolute temperature, respectively [4].

Gating properties of ryanodine receptor (RyR) on intracellular calcium stores can be described as follows:

$$\begin{aligned} dP_{C1}/dt &= -K_a^+ [Ca^{2+}]_i^n + K_a^- Po_1 \\ dPo_2/dt &= K_b^+ [Ca^{2+}]_i^m Po_1 - K_b^- Po_2 \\ dP_{C2}/dt &= K_c^+ Po_1 - K_c^- P_{C2} \\ Po_1 + Po_2 + P_{C1} + P_{C2} &= 1 \end{aligned} \quad (6)$$

where C_1 and C_2 are closed states whereas O_1 and O_2 are open states of RyR; $K_i^{\pm}$ ($i = a, b, c$) are rate constants of transitions between states [14].

Ca^{2+} flux across the internal Ca^{2+} stores (endoplasmic reticulum, ER) can be described as follows:

$$\frac{[Ca^{2+}]_{er}}{dt} = -f_{er} \cdot (V_{cyt}/V_{er}) \cdot (ER_{ryr} - ER_{fil} + ER_{leak}) \quad (7)$$

where V_{cyt} and V_{er} represent the cell volume (excluding ER) and the ER volume, respectively; f_{er} is the Ca^{2+} buffering coefficient of ER; ER_{ryr} denotes the RyR-mediated Ca^{2+} release; ER_{fil} represents the active pumping through the ER Ca^{2+}-ATPase; ER_{leak} represents a passive leak process [3].

ER_{ryr}, ER_{fil} and ER_{leak} are further described as follows:

$$\begin{aligned} ER_{ryr} &= v_{ryr} \cdot (Po_1 + Po_2) \cdot ([Ca^{2+}]_{er} - [Ca^{2+}]_i) \\ ER_{fil} &= v_{fil} \cdot [Ca^{2+}]_i^2 / ([Ca^{2+}]_i^2 + K_{fil}^2) \\ ER_{leak} &= v_{leak} \cdot ([Ca^{2+}]_{er} + [Ca^{2+}]_i) \end{aligned} \quad (8)$$

Voltage-gated Na^+ conductance and three types of K^+ conductance (delay time rectifying K^+ current, outward rectifying K^+ current, anomalous rectifying K^+ current) are described following a previously reported model [15,16].

Parameter values for the above equations used in our simulations are listed in Table 1. These values are inferred from the original work describing specific equations. The biophysical properties of H1 cells for simulation of membrane potential changes are also included.

Acknowledgements

This work was supported by grants from the National Foundation of Natural Science of China (No. 60775034). The authors are grateful to Prof. Y.H. Ji and Dr. X.H. Feng for helpful discussion and technical assistance.

References

1. Carafoli E. Calcium signaling: a tale for all seasons. *Proc Natl Acad Sci U S A* 2002; **99**:1115–1122.
2. Field GD, Chichilnisky EJ. Information processing in the primate retina: circuitry and coding. *Annu Rev Neurosci* 2007; **30**:1–30.
3. Huang SY, Liu Y, Liang PJ. Role of Ca^{2+} store in AMPA-triggered Ca^{2+} dynamics in retinal horizontal cells. *Neuroreport* 2004; **15**:2311–2315.
4. Hayashida Y, Yagi T. On the interaction between voltage-gated conductances and Ca^{2+} regulation mechanisms in retinal horizontal cells. *J Neurophysiol* 2002; **87**:172–182.
5. Watkins JC, Jane DE. The glutamate story. *Br J Pharmacol* 2006; **147**: S100–S108.
6. Yang XL. Characterization of receptors for glutamate and GABA in retinal neurons. *Prog Neurobiol* 2004; **73**:127–150.
7. Shen Y, Zhang M, Jin Y, Yang XL. Functional *N*-methyl-D-aspartate receptors are expressed in cone-driven horizontal cells in carp retina. *Neurosignals* 2006; **15**:174–179.
8. Lu T, Yang XL. Carp retinal horizontal cells: dissociation, morphology and physiological characteristics. *Chin J Neuroanat* 1995; **11**:299–306.
9. Carnevale T, Hines M. *The NEURON book*. Cambridge, UK: Cambridge University Press; 2006.
10. Tachibana M. Ionic currents of solitary horizontal cells isolated from goldfish retina. *J Physiol* 1983; **345**:329–351.
11. McBain CJ, Mayer ML. *N*-methyl-D-aspartic acid receptor structure and function. *Physiol Rev* 1994; **74**:723–760.
12. Shen W, Jiang Z. Characterization of glycinergic synapses in vertebrate retinas. *J Biomed Sci* 2007; **14**:5–13.
13. Destexhe A, Mainen ZF, Sejnowski TJ. An efficient method for computing synaptic conductances based on a kinetic model of receptor binding. *Neural Comput* 1994; **6**:14–18.
14. Keizer J, Levine L. Ryanodine receptor adaptation and Ca^{2+}-induced Ca^{2+} release-dependent Ca^{2+} oscillations. *Biophys J* 1996; **71**: 3477–3487.
15. Usui S, Kamiyama Y, Ishii H, Ikeno H. Reconstruction of retinal horizontal cell responses by the ionic current model. *Vision Res* 1996; **36**:1711–1719.
16. Wang XL, Jin X, Liang PJ. Modeling the pre- and post-synaptic components involved in the synaptic modification between cones and horizontal cells in carp retina. *Biol Cybern* 2007; **96**:367–376.